Photo-Fenton and oxygen vacancies synergy for enhancing catalytic activity with S-scheme FeS_2/Bi_2WO_6 heterostructure

Jin Ye,‡[a] Yuanyuan Zhang,‡[b] Juan Wang,[c] Shuang Liu,[a] Yuanhang Chang,[a] XiuPing Xu,[a] Chunte Feng,[a] Jian Xu,[a,d] Li Guo,*[b] Jiating Xu,*[ae] and Yujie Fu[a]

[a] *Key Laboratory of Forest Plant Ecology, Ministry of Education, College of Chemistry, Chemical Engineering and Resource Utilization, Northeast Forestry University, Harbin, 150040, P. R. China*

[b] *Shaanxi Key Laboratory of Chemical Reaction Engineering, School of Chemistry & Chemical Engineering, Yan'an University, Yan'an 716000, China, P. R. China*

[c] *School of Chemistry & Chemical Engineering, Linyi University, Linyi 276000, P. R. China*

[d] *Qiqihaer Branch of Heilongjiang Academy of Agricultural Sciences, 10060, Qiqihaer*

[e] *Heilongjiang Provincial Key Laboratory of Ecological Utilization of Forestry-Based Active Substances, Northeast Forestry University, Harbin, 150040, P. R. China*

1. Experimental section

1.1. Materials

Sodium hydroxide (NaOH, 96.0%), Iron (III) chloride hexahydrate ($FeCl_3 \cdot 6H_2O$, 99.0%) and cetyltrimethylammonium bromide (CTAB) were purchased from Tianjin Kemiou Chemical Reagent Co., Ltd (Tianjin, China). Sodium tungstate dihydrate ($Na_2WO_4 \cdot 2H_2O$, 99.5%), bismuth nitrate pentahydrate ($Bi(NO_3)_3 \cdot 5H_2O$, 99%), and anhydrous ethanol (C_2H_5OH, 99.7%) were purchased from Tianjin Zhiyuan Chemical Reagent Co., Ltd (Tianjin, China). Hydrochloric acid (HCl, 36%), nitric acid (HNO_3, 63%) and ammonia solution ($NH_3 \cdot H_2O$, 28%) were purchased form Sichuan Xilong chemical Co., Ltd (Sichuan, China). Thiourea (CH_4N_2S, 99.0%) was purchased from Sinopharm Chemical Reagent Co., Ltd (Shanghai, China). The deionized water was used as a solvent. All the reagents were of analytical grade and were used without any further purification.

1.2 Characterization of the as-prepared samples

X-ray powder diffractometer (Shimadzu XRD-7000) was used to analyze the crystallographic properties of the catalysts. Fourier-transform infrared spectra (FT-IR) were performed on NicoletiS10. X-ray photoelectron spectroscopy (XPS) was obtained at PHI-5400 (America PE) 250 xi system. The morphology of the sample was analyzed by scanning electron microscope (SEM, JSM-6700F) and transmission electron microscope (JEM-2100) (Japan electronics). Energy disperse X-ray (EDX) was performed on a field emission scanning electron microscope (JSM-7610F) to analyze elemental features of the samples. The UV-Vis diffuse reflectance spectra

(UV-Vis-DRS) were measured on UV-2550 UV-Vis Spectrophotometer. The electron spin resonance (ESR) spectra were examined on a Bruker ELEXSYS-II E500 CW-EPR. Photoluminescence (PL) spectroscopy was recorded *via* an Agilent Cary Eclipse (F-7000) at room temperature. Fourier-transform infrared spectra (FT-IR) were performed on NicoletiS10. Time-resolved photoluminescence (TRPL) spectra were conducted on a FLS920 fluorescence spectrometer (Edinburgh Analytical Instruments, UK). The chemical composition and element valence were analyzed using X-ray photoelectron spectroscopy (XPS, Kratos Axis Ultra) with a monochromated Al Kα X-ray source (hν=1486.6 eV). N_2 adsorption-desorption isotherm measurements were investigated to study the Brunauer-Emmett-Teller (BET) specific surface areas of the samples. All electrochemical and photoelectrochemical characterizations were performed on an electrochemical workstation (CHI760E) using a three-electrode system (pH 7.0) with Pt as the counter electrode, Ag/AgCl as the reference electrode, and indium tin oxide (ITO) as the working electrode under visible light. Transient photocurrent response measurements were tested on an electrochemical workstation in the saturated solution of Na_2SO_4 (0.5 M) with 20 s interval under visible light by controlling the light on and off. Electrochemical impedance spectroscopy (EIS) was carried out in the frequency range of 0.01 to 10^5 Hz by electrochemical workstation with Nafion solution. And Ultraviolet photoemission spectroscopy (UPS) measurements were performed on a Thermo Fisher ESCALAB 250Xi instrument with a He radiation source (hν = 21.22 eV). From UPS spectra, the work function (Φ) of

sample was calculated according to the equation $\Phi = h\nu - E_{Fermi} + E_{Cutoff}$, in which $h\nu$ is the He I energy (21.22 eV).

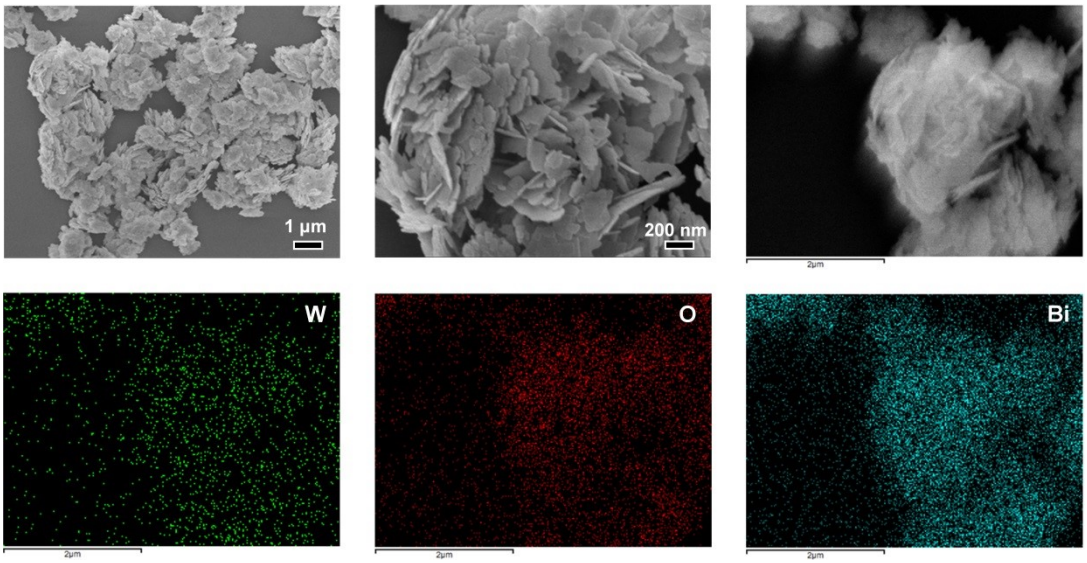

Fig. S1. The SEM images and the corresponding elements mapping of Bi_2WO_6-OVs.

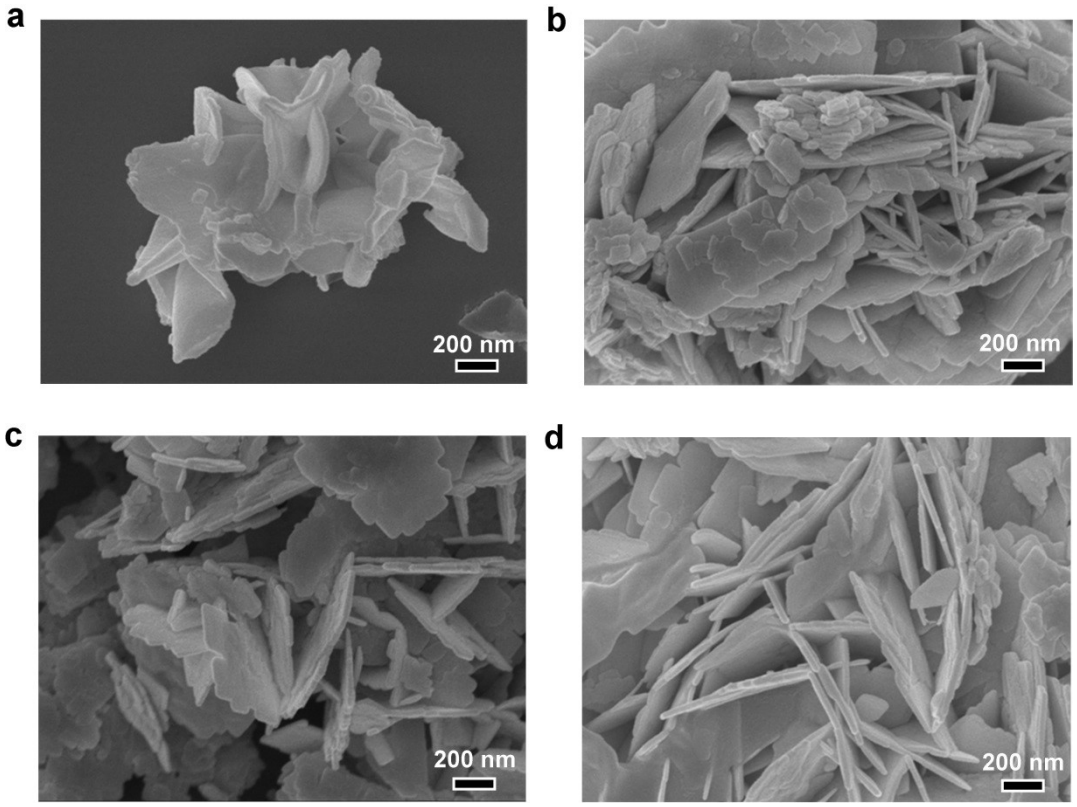

Fig. S2. The SEM images of (a) pure Bi_2WO_6, (b) 0.5%FeS_2/Bi_2WO_6, (c) 1%FeS_2/Bi_2WO_6 and (d) 2%FeS_2/Bi_2WO_6.

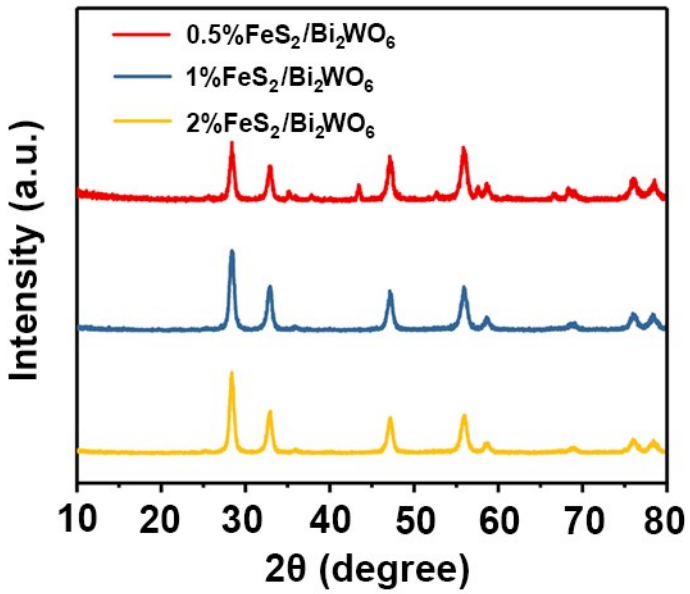

Fig. S3. XRD patterns of 0.5%FeS_2/Bi_2WO_6, 1%FeS_2/Bi_2WO_6 and 2%FeS_2/Bi_2WO_6.

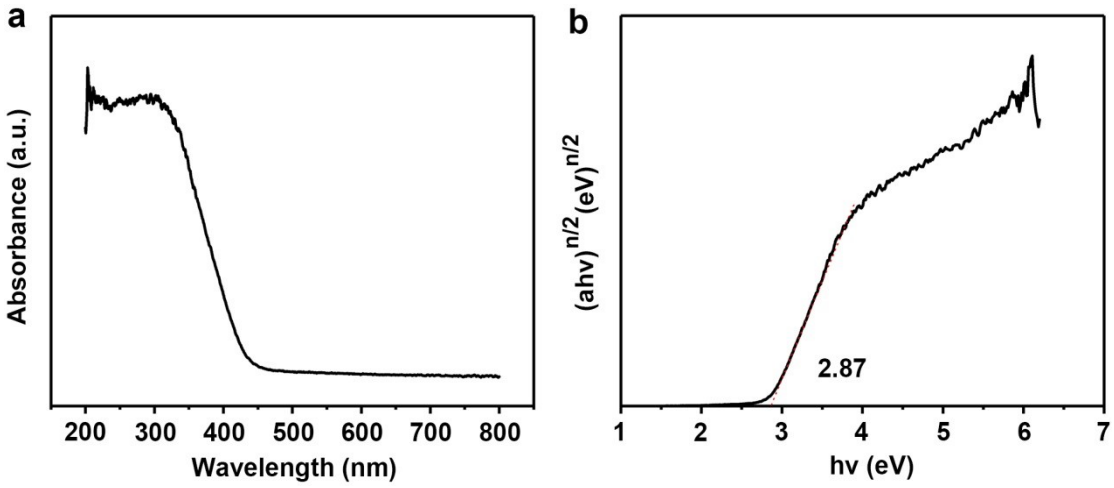

Fig. S4. UV-vis diffuses absorbance spectra (a) and the corresponding plots of $(\alpha h\nu)^{n/2}$ (b) for pure Bi_2WO_6.

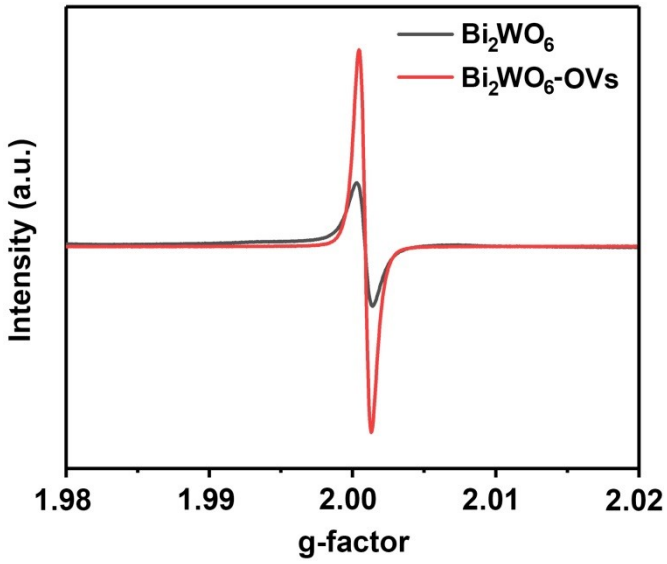

Fig. S5. ESR spectra of pure Bi_2WO_6 and Bi_2WO_6 -OVs.

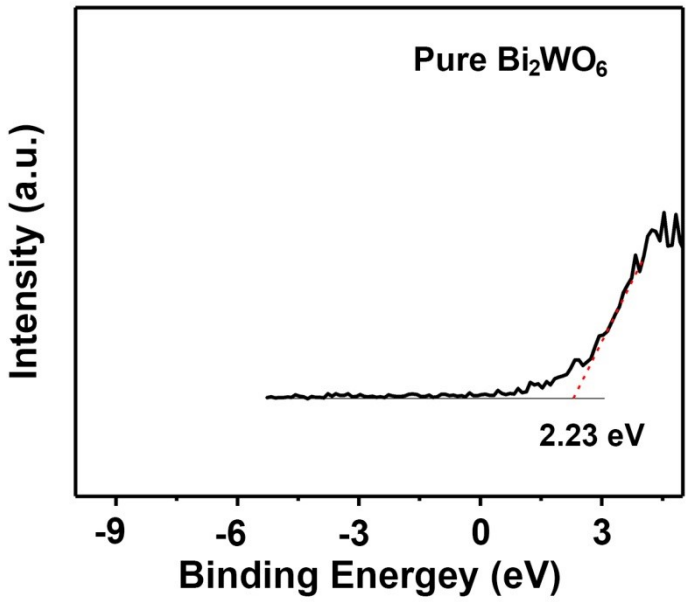

Fig. S6. The valence XPS spectrum for pure Bi_2WO_6.

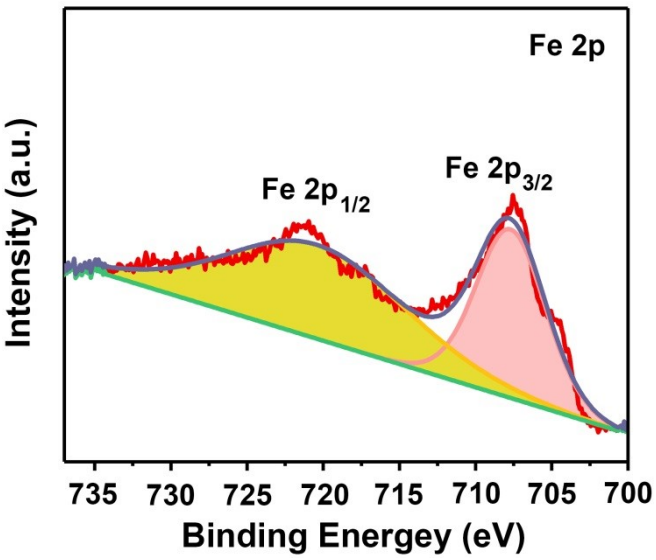

Fig. S7. The high-resolution spectrum of Fe 2p for 1%FeS_2/Bi_2WO_6 catalyst.

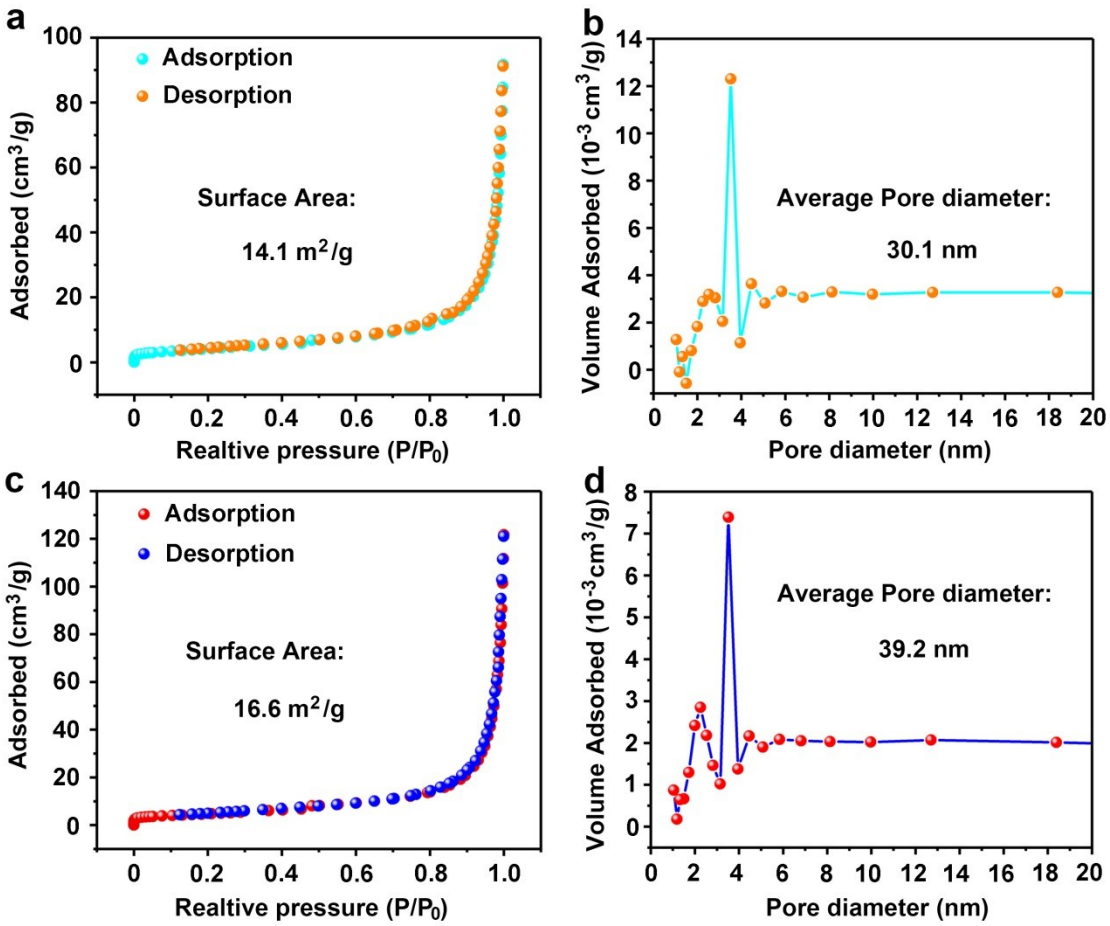

Fig. S8. N_2 adsorption-desorption isotherms and average pore diameter of (a-b) 1%FeS_2/Bi_2WO_6 and (c-d) Bi_2WO_6 -OVs.

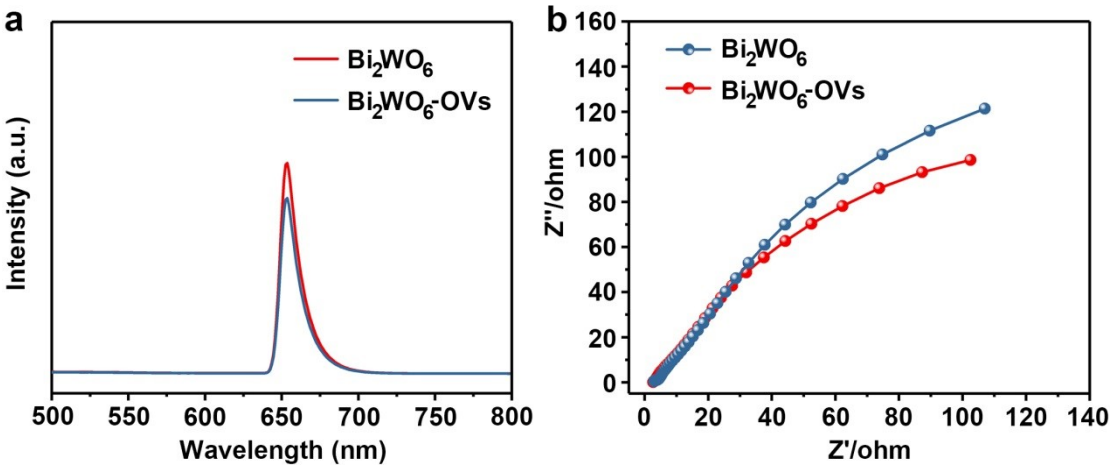

Fig. S9. Photoluminescence (a) and electrochemical impedance (b) spectra for pure Bi_2WO_6 and Bi_2WO_6 -OVs.

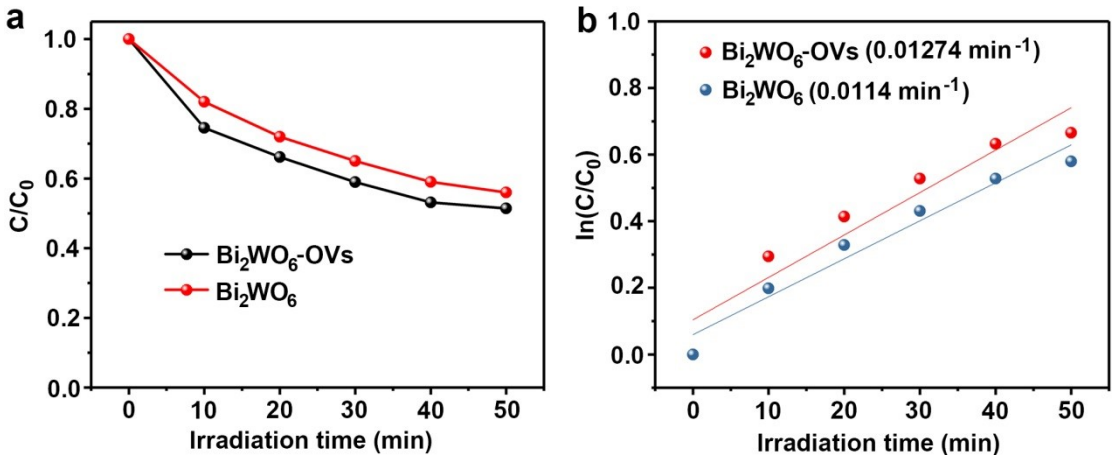

Fig. S10. Photocatalytic activity of degradation of TC-HCl (a) under visible light irradiation and the corresponding kinetics rate of degradation of TC-HCl (b) for pure Bi_2WO_6 and Bi_2WO_6 -OVs.

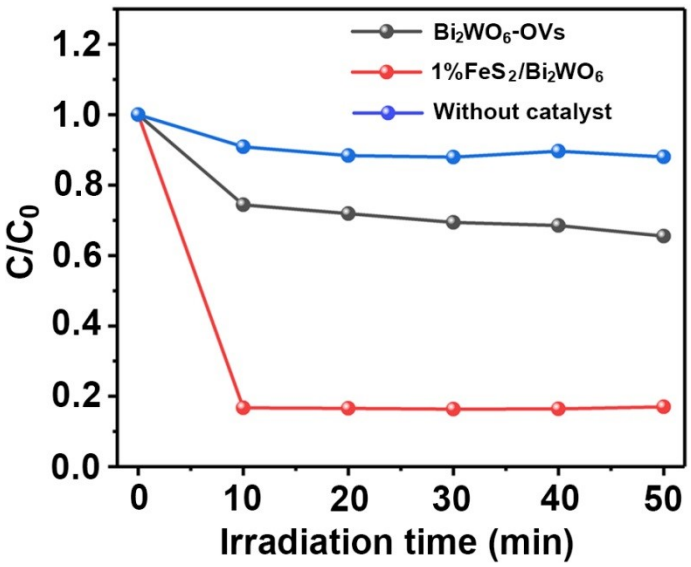

Fig. S11. Fenton activity of degradation of TC-HCl upon different catalysts.

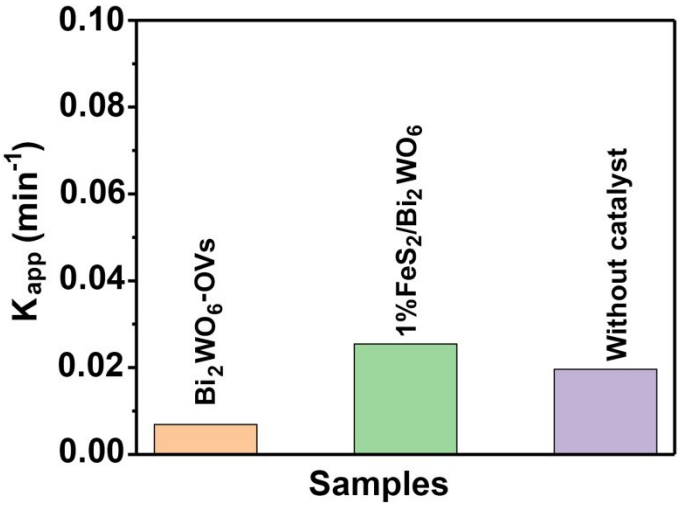

Fig. S12. Fenton activity of degradation of TC-HCl with different catalysts.

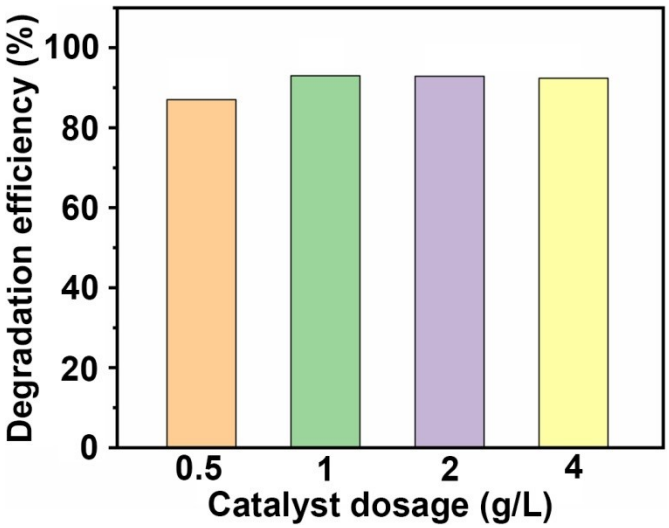

Fig. S13. Degradation efficiency of TC-HCl with different concentrations of catalyst dosage.

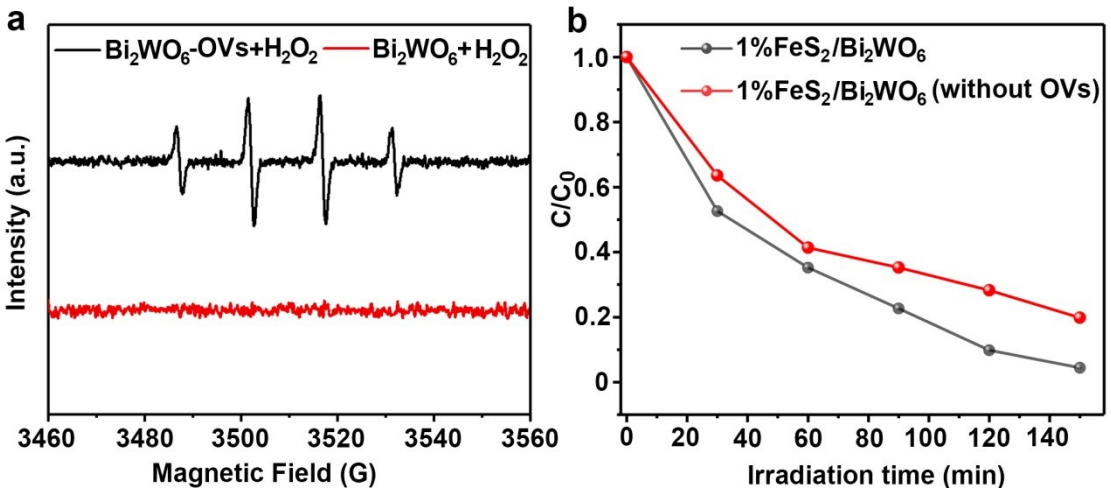

Fig. S14. ESR spectra of pure Bi_2WO_6 and Bi_2WO_6-OVs for ·OH with H_2O_2 (a) and photo-Fenton activity of degradation of TC-HCl for 1%FeS_2/Bi_2WO_6 without or with oxygen vacancies (b).

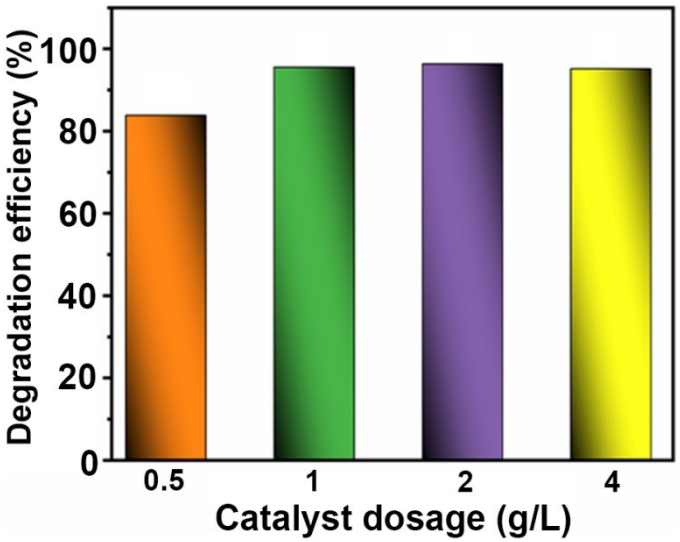

Fig. S15. Degradation efficiency of RhB with different concentrations of catalyst dosage.

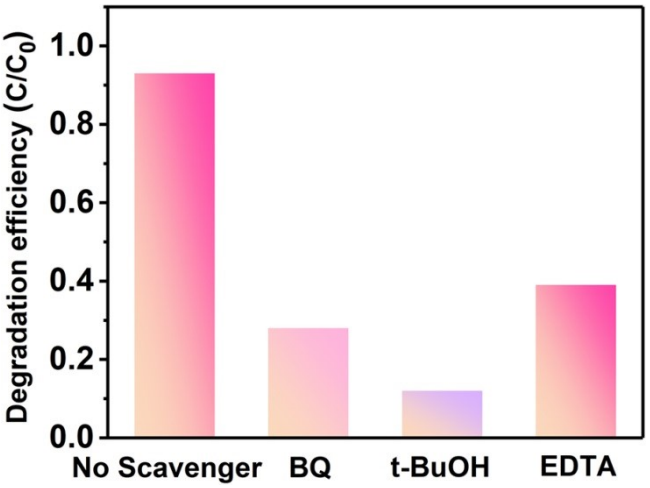

Fig. S16. Photocatalytic activity of 1%FeS_2/Bi_2WO_6 in the presence of different scavengers.

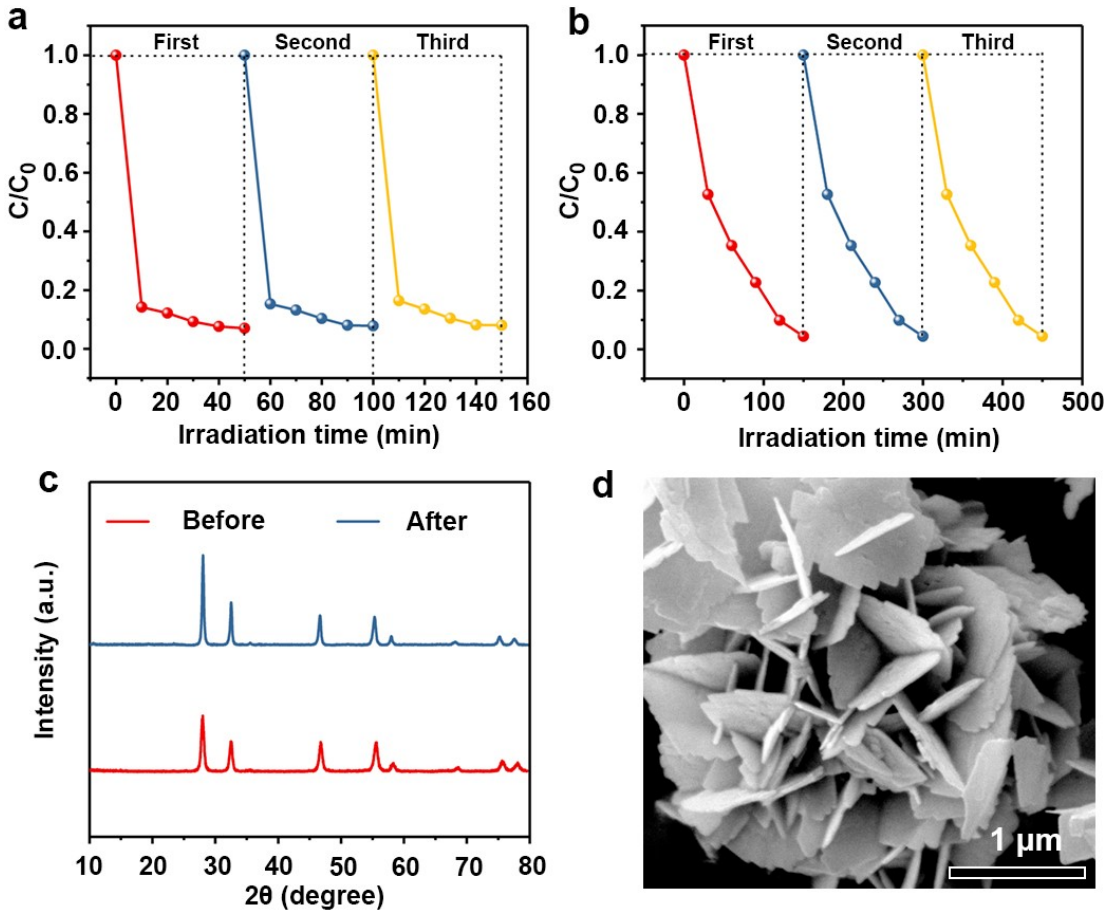

Fig. S17. The three cycling experiments of photo-Fenton activity of degradation of TC-HCl (a) and RhB (b), XRD patterns for 1%FeS_2/Bi_2WO_6 before and after recycling (c), and the SEM image of 1%FeS_2/Bi_2WO_6 catalyst after reaction (d).

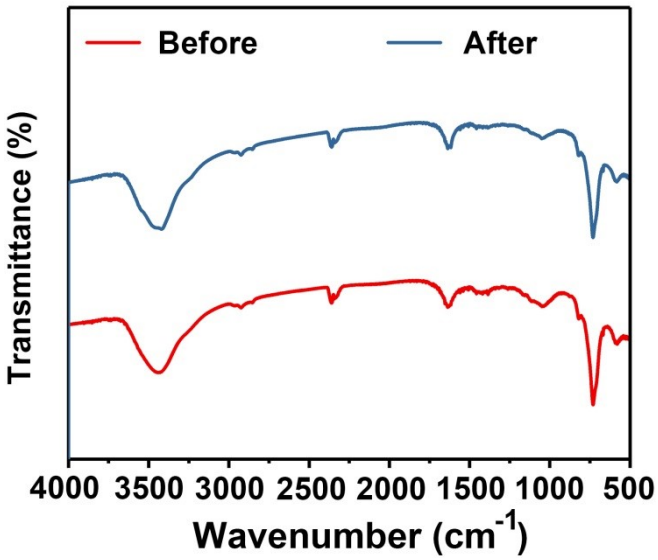

Fig. S18. The FT-IR spectra of the 1%FeS_2/Bi_2WO_6 before and after the catalytic reaction.

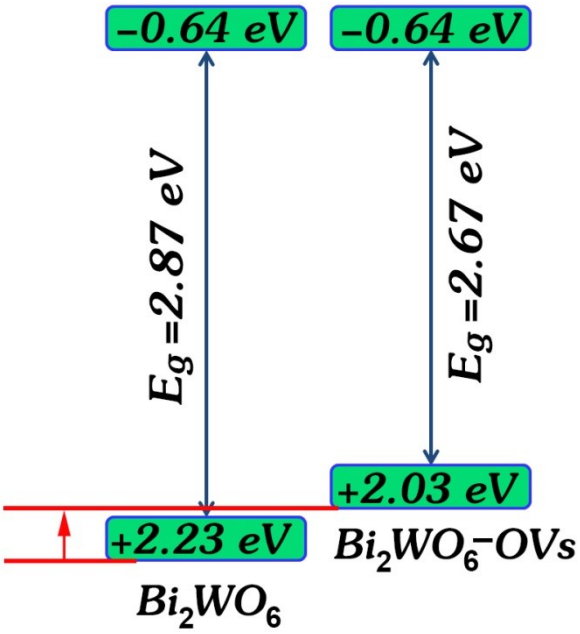

Fig. S19. The energy band positions of pure Bi_2WO_6 and Bi_2WO_6-OVs.

Table S1. The specific surface area and average pore diameter for Bi_2WO_6-OVs and 1%FeS_2/Bi_2WO_6.

Samples	BET surface area (m^2/g)	Average pore diameter (nm)
Bi_2WO_6-OVs	16.6	39.2
1%FeS_2/Bi_2WO_6	14.1	30.1

Table S2. Comparison of photocatalytic activity over Bi_2WO_6-based materials.

Catalysts	Light source	Pollutant	Rate constant (k/min^{-1})	Ref.
2D biomimetic Bi_2WO_6	Simulated Solar Light	TC-HCl	0.03300	1
g-C_3N_4/Bi_2WO_6/AgI	Visible Light	TC-HCl	0.03500	2
Br/Bi_2WO_6	Visible Light	RhB	0.01700	3
MIL-125(Ti)/Bi_2WO_6	Visible Light	TC-HCl	0.01800	4
1%FeS_2/Bi_2WO_6	Visible Light	TC-HCl	0.04430	This Work
1%FeS_2/Bi_2WO_6	Visible Light	RhB	0.02007	This Work

Table S3. The TRPL decay data of Bi_2WO_6-OVs and 1%FeS_2/Bi_2WO_6.

Samples	τ_1 (ns)	A_1	τ_2 (ns)	A_2	$\tau_{average}$ (ns)
1%FeS_2/Bi_2WO_6	0.5359	4.65×10^8	4.44	3.7395	0.5359
Bi_2WO_6-OVs	0.9481	4.97×10^4	0.9485	4.96×10^4	0.9483

References

[1] H. Yi, M. Yan, D. Huang, G. Zeng, C. Lai, M. Li, X. Huo, L. Qin, S. Liu, X. Liu, B. Li, H. Wang, M. Shen, Y. Fu and X. Guo, *Appl. Catal. B Environ.,* 2019, **250**, 52-62.

[2] W. Xue, D. Huang, J. Li, G. Zeng, R. Deng, Y. Yang, S. Chen, Z. Li, X. Gong and B. Li, *Chem. Eng. J.,* 2019, **373**, 1144-1157.

[3] R.R. Song, N.H. Chen, B. Han, S.H. Yu, Y. Wang, K. Liu, Z.F. Tong and H.B. Zhang, *Environ. Sci. Pollut. Res. Int.,* 2021, **28**, 36434-36452.

[4] S. Yin, Y. Chen, C. Gao, Q. Hu, M. Li, Y. Ding, J. Di, J. Xia and H. Li, *J. Photoch. Photobiol. A*, 2020, **387**, 112149.